Using Activated Transport in Parallel Nanowires for Energy Harvesting and Hot Spot Cooling

Riccardo Bosisio, Cosimo Gorini, Geneviève Fleury, Jean-Louis Pichard

Using Activated Transport in Parallel Nanowires for Energy Harvesting and Hot Spot Cooling

Riccardo Bosisio, Cosimo Gorini, Geneviève Fleury and Jean-Louis Pichard
Service de Physique de l'État Condensé (CNRS URA 2464), IRAMIS/SPEC, CEA Saclay, 91191 Gif-sur-Yvette, France

We study the thermoelectric effects in arrays of disordered nanowires in parallel, at temperatures where charge transport between localized states is thermally assisted by phonons. We obtain large power factors and electrical figures of merit, when the chemical potential probes the band edges of the nanowires, the large thermopowers self-averaging while the small electrical conductances add. The role of the parasitic phonon heat transport is estimated. We also show that phonon absorption and emission occur at opposite ends of the array in band-edge transport, a phenomenon which could be exploited for cooling hot spots in electronic circuits.

A good thermoelectric machine must be efficient at converting heat into electricity and also provide a substantial electric output power for practical applications. In the linear response regime, this requires optimizing simultaneously the figure of merit $ZT = S^2GT/(K^e+K^{ph})$ and the power factor $\mathcal{Q} = S^2G$, T being the operating temperature, S the device thermopower, G its electrical conductance, and K^e and K^{ph} its electronic and phononic thermal conductances. In the quest for high performance thermoelectrics, semiconductor nanowires (NWs) are playing a front role [1–6], apparently offering the best of three worlds. First, an enhanced S due to strongly broken and gate-tunable particle-hole symmetry [4, 7–9]. Second, a suppressed K^{ph} by virtue of reduced dimensionality [2, 3]. Finally, a high power output thanks to scalability, i.e. parallel stacking [2, 5, 10–17].

In this letter, we study arrays of doped semiconductor NWs, arranged in parallel and attached to two electrodes. The NWs are either suspended or deposited onto an electrically and thermally insulating substrate. A metallic gate beneath the sample is used to vary the carrier density inside the NWs. This setup is referred to as field effect transistor (FET) configuration and is sketched in Fig. 1. If the thermopower or the thermal conductances are to be investigated, a heater (not shown in Fig. 1) is added on one side of the sample to induce a temperature gradient between the electrodes. We focus on the phonon-assisted activated regime and assume *(i)* that transport takes place in the NWs impurity band only and *(ii)* that the substrate, or the NWs themselves if they are suspended, act as a phonon bath to which NWs charge carriers are well coupled. We thus consider intermediate temperatures, where the thermal energy k_BT is high enough to allow inelastic hopping between localized states of different energies (typically a few Kelvin degrees), yet low enough to neglect the possible presence of other bands (typically tens of Kelvin degrees in weakly doped crystalline semiconductors up to room temperature in amorphous materials) [18]. Following Refs. [19–21], we solve numerically the Miller-Abrahams random resistor network problem [22] to obtain S, G, and K^e.

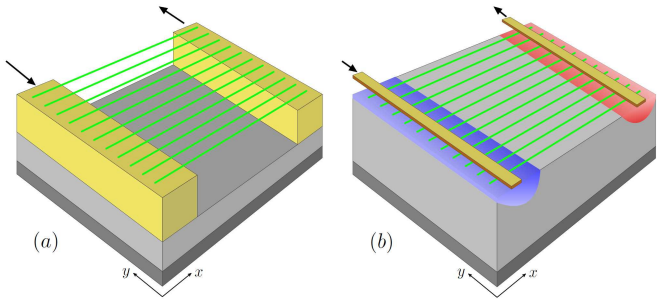

FIG. 1. (Color online) Array of suspended (a) and deposited (b) parallel NWs in the FET configuration. The NWs are drawn in green, the two metallic electrodes in yellow, the substrate in grey and the back gate in dark grey. The blue [red] spot in (b) indicates the substrate region that is cooled down [heated up] in the phonon-assisted activated regime, when a charge current flows from the left to the right electrode and the gate voltage is tuned so as to probe the lower edge of the NWs impurity band.

This allows us to identify also the regions where heat exchanges dominantly take place.

We find that once a large set of NWs is stacked in parallel, the strong G, S and K^e fluctuations are suppressed. Denoting by G_0, S_0 and K_0^e the *typical* values for a single NW, we observe more precisely (see Supplemental Material) that the thermopower of a large NW array self-averages ($S \to S_0$) while its electrical and electronic thermal conductances $G \to MG_0$, $K^e \to MK_0^e$ as the number M of wires in parallel increases. Taking full advantage of the gate, we move close to the impurity band edges, where we recently obtained a drastic S_0 enhancement [21]. We show that in this regime a large S_0 partly compensates an exponentially small G_0, so that substantial values of the power factor $\mathcal{Q} \approx MS_0^2G_0$ can be reached upon stacking plenty of NWs in parallel (see Fig. 2). Remarkably, the electrical figure of merit $Z_eT = S^2GT/K^e$ is also found to reach promising values $Z_eT \approx 3$ when $\mathcal{Q}$ is maximal. Furthermore, we discuss how the phononic thermal conductance K^{ph} will inevitably reduce the full figure of merit ZT and argue that,

even if record high ZT is probably not to be sought in such setups, the latter have the great advantage of offering at once high output power and reasonable efficiency with standard nanotechnology building blocks. On the other hand, we will also show at the end of the letter how deposited NWs in the FET configuration can be used to generate hot/cold spots "on demand". The idea is simple to grasp: When the gate voltage is adjusted such that the equilibrium electrochemical potential μ (defined in the electronic reservoirs) roughly coincides with one (say the lower) impurity band edge, basically all energy states in the NWs lie above μ. Therefore, if charge carriers injected into the system around μ are to gain the other end, they need to (on the average) absorb phonons at the entrance so as to jump to available states, and then to release phonons when tunneling out (again at μ). This generates a cold and a hot spot in the nearby substrate regions (see Figs. 1(b) and 3) that get scrambled in the absence of the gate voltage. Such reliable and tunable cold spots may be exploited in devising thermal management tools for high-density circuitry, where ever increasing power densities have become a critical issue [23].

Let us remark that parallel NW arrays can nowadays be realized in different manners and with numerous materials [11–14, 16, 17]. Architecture and/or material specific predictions, though very important for practical engineering purposes, are however *not* our concern at present. On the contrary, our goal is to reach conclusions which are as general as possible, relying on a bare-bone but widely applicable model devised to capture the essentials of the physics we are interested in.

Model and method. Each NW is modeled as a chain of length L described by a tight-binding Hamiltonian with on-site disorder:

$$\mathcal{H} = -t \sum_{i=1}^{N-1} \left(c_i^\dagger c_{i+1} + \text{h.c.} \right) + \sum_{i=1}^{N} (\epsilon_i + V_g) c_i^\dagger c_i \,. \qquad (1)$$

Here N is the number of sites in the chain ($L = Na$ with a lattice spacing), $c_i^\dagger$ and c_i are the electron creation and annihilation operators on site i and t is the hopping energy (*inter*-wire hopping is neglected). We assume that no site can be doubly occupied due to Coulomb repulsion, but otherwise neglect interactions [24]. The site energies ϵ_i are uncorrelated random numbers uniformly distributed in the interval $[-W/2, W/2]$, while V_g is the constant gate potential. The electronic states are localized at certain positions x_i with localization lengths ξ_i and eigenenergies E_i. For simplicity's sake, we generate randomly the positions x_i along the chain (with a uniform distribution) and assume $\xi_i = \xi(E_i)$, where $\xi(E)$ characterizes the exponential decay of the *typical* conductance $G_0 \sim \exp(-2L/\xi)$ at zero temperature and energy E.

The NWs are attached to two electronic reservoirs L and R, and to a phonon bath, i.e. the system is in a three-terminal configuration. Particles and heat(energy) can be exchanged with the electrodes, but only heat(energy) with the phonon bath. At equilibrium the whole system is thermalized at a temperature T and both L and R are at electrochemical potential μ (set to $\mu \equiv 0$, at the band center when $V_g = 0$). A voltage and/or temperature bias between the electrodes drives an electron current through the NWs. Hereafter we consider the linear response regime, valid when small biases $\delta\mu \equiv \mu_L - \mu_R$ and $\delta T \equiv T_L - T_R$ are applied.

We study the inelastic activated regime [20, 21]. Charge carriers (say electrons of charge e) tunnel elastically from reservoir $\alpha = L, R$ into some localized states i whose energies E_i are located in a window of order $k_B T_\alpha$ around μ_α. They then proceed via phonon-assisted hops to the other end, finally tunneling out. The carriers' hop along the NWs is of the order of Mott's length L_M in space and Mott's energy Δ in energy [21]. At the lowest temperatures considered in this work, $\xi(\mu) \ll L_M \ll L$ and transport is of Variable Range Hopping (VRH) type. An increasing temperature shortens L_M until $L_M \approx \xi(\mu)$, when the Nearest Neighbors Hopping (NNH) regime is reached. The crossover VRH→NNH takes place roughly at Mott's temperature T_M, whose dependence on V_g can be found in Ref. [21].

The electron and heat currents are calculated by solving the random resistor network problem [22, 24]. The method is summarized in the Supplemental Material. It takes as input parameters the rate γ_e quantifying the coupling between the NWs' (localized) and the reservoirs' (extended) states, and the rate γ_{ep} measuring the coupling to the NWs and/or substrate phonons. We point out that we go beyond the usual approximation [20, 22, 24] neglecting the ξ_i's variations from state to state ($\xi_i \approx \xi(\mu)$), the latter being inappropriate close to the band edges, where ξ_i varies strongly with the energy. Following Ref. [21] the random resistor network is then solved for $\xi_i \neq \xi_j$. The particle and heat currents thus obtained are related to the small imposed biases $\delta\mu, \delta T$ via the Onsager matrix [25], which gives access to G, K^e and S.

Power factor and figure of merit. By stacking a large number M of NWs in parallel, the device power factor can be enhanced $\mathcal{Q} \approx M S_0^2 G_0$ *without* affecting its electrical figure of merit $Z_e T \approx S_0^2 G_0 T / K_0^e$. Fig. 2 shows how the asymptotical $\mathcal{Q}/M$ and $Z_e T$ values (reached when $M > M^* \approx 100$) depend on the gate voltage V_g and on the temperature T. We observe in panel (a) that the power factor is maximum for μ close the impurity band edge (black solid line) and for VRH temperatures. This parameter range represents the best compromise between two opposite requirements: maximizing the thermopower (hence favoring low T and large V_g) while keeping a reasonable electrical conductance (favoring instead higher T and $V_g \approx 0$). Formulas previously reported [21], giving the T- and V_g-dependence of G_0 and S_0, let us predict that $\mathcal{Q}$ is maximal when

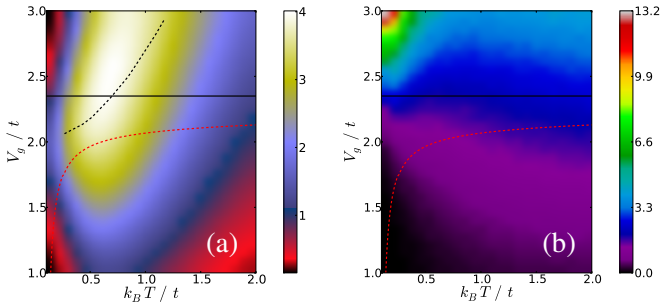

FIG. 2. (Color online) $\mathcal{Q}/M$ in unit of $k_B^2/\hbar$ (a) and Z_eT (b) as a function of T and V_g. Data are shown in the large M limit ($M = 150$) where there is self-averaging. The horizontal lines give V_g's value at which the band edge is probed at μ (below [above] it, one probes the inside [outside] of the impurity band). The red dashed lines $T = T_M$ separate the VRH ($T \lesssim T_M$) and the NNH ($T \gtrsim T_M$) regimes. The black dashed line in (a) is the contour along which $S_0 = 2k_B/e$. Parameters: $W = t$, $\gamma_e = \gamma_{ep} = t/\hbar$ and $L = 450a$.

$|S_0| = 2k_B/|e| \approx 0.2\,\mathrm{mV\,K^{-1}}$ (black dashed line). A comparison between panels (a) and (b) of Fig. 2 reveals that, in the parameter range corresponding to the best power factor ($V_g \sim 2.5t, k_BT \sim 0.6t$), $Z_eT \simeq 3$, a remarkably large value. Much larger values of Z_eT could be obtained at lower temperatures or far outside the band, but they are not of interest for practical purposes since in those regions $\mathcal{Q}$ is vanishing. In the Supplemental Material, $\mathcal{Q}$ and Z_eT are shown to be roughly independent of the NWs length L, in the temperature and gate voltage ranges explored in Fig. 2. Moreover $\mathcal{Q}/\gamma_e$ and Z_eT are almost independent of the choice of the parameters γ_e and γ_{ep}, provided $\gamma_{ep} \gtrsim \gamma_e$. When $\gamma_{ep} < \gamma_e$, both quantities are found to be (slightly) reduced. Thus, we argue that the numerical results shown in Fig. 2 can be addressed at a semi-quantitative level.

Let us now estimate the order-of-magnitude of the device's performance. The substrate (or the NWs themselves if they are suspended) is assumed to supply enough phonons to the NWs charge carriers for the condition $\gamma_{ep} \gtrsim \gamma_e$ to hold. Besides, we keep explicit the γ_e-linear dependence of $\mathcal{Q}$ (and of K_0^e that will soon be needed). γ_e depends on the quality of the metal/NW contact. We estimate it to be within the range $0.01 - 1$ in units of $t/\hbar$, where $t/k_B \approx 150\,\mathrm{K}$ throughout [26]. This yields $\gamma_e \approx 0.02 - 2 \times 10^{13}\,\mathrm{s^{-1}}$. For the sake of brevity, we introduce the dimensionless number $\tilde{\gamma}_e = \gamma_e\hbar/t$. Focusing on the region of Fig. 2(a) where the power factor is maximal, we evaluate the typical output power and figure of merit than can be expected. We first notice that power factor $\mathcal{Q}/M \approx 4k_B^2/h$ maximum values in Fig. 2(a), obtained with $\tilde{\gamma}_e = 1$, would yield $\mathcal{Q} \approx 7\tilde{\gamma}_e \times 10^{-7}\,\mathrm{W.K^{-2}}$ for a 1-cm wide chip with $M \approx 10^5$ parallel NWs. Since $\mathcal{Q}$ controls the maximal output power P_{max} that can be extracted from the setup as $P_{max} = \mathcal{Q}(\delta T)^2/4$ [27], one expects $P_{max} \approx 20\tilde{\gamma}_e\,\mu\mathrm{W}$ for a small temperature bias $\delta T \approx 10\,\mathrm{K}$. In this region a large value $Z_eT \approx 3$ is obtained, but to estimate the full figure of merit $ZT = Z_eT/(1+K^{ph}/K^e)$, the phononic part K^{ph} of the thermal conductance must also be taken into account. To limit the reduction of ZT by phonons, the setup configuration with suspended nanowires is preferable (Fig. 1(a)). In this case $K^{ph} \approx MK_0^{nw}$, K_0^{nw} being the typical phononic thermal conductance of a single NW, and has to be compared to $K^e \approx MK_0^e$. Introducing the corresponding conductivities κ's, the ratio $K^{ph}/K^e \approx \kappa_0^{nw}/\kappa_0^e$ is to be estimated. Our numerical results show $K_0^e \approx 1.5\tilde{\gamma}_e k_B t/\hbar$ in the range of interest where $\mathcal{Q}$ is maximal and $Z_eT \approx 3$ (at $V_g = 2.5t$ and $k_BT = 0.6t$, keeping other parameters in Fig. 2 unchanged). For a NW of length $1\,\mu$m and diameter 20 nm, this yields $\kappa_0^e \approx 1\tilde{\gamma}_e\,\mathrm{W/(K.m)}$. The measured thermal conductivity of Si NWs of similar geometry is $\kappa_0^{nw} \approx 2\,\mathrm{W/(K.m)}$ at $T \approx 100\,\mathrm{K}$ [28]. We thus evaluate for suspended NWs $ZT \approx Z_eT/(1 + 2/\tilde{\gamma}_e)$, i.e. $ZT \approx 0.01 - 1$ for $Z_eT \approx 3$ and $\tilde{\gamma}_e = 0.01 - 1$. Those estimations though rough are extremely encouraging as they show us that such a simple and Si-based device shall generate high electrical power from wasted heat (scalable with $M \gtrsim M^*$) with a correct efficiency (independent of $M \gtrsim M^*$).

Let us note that maximizing γ_e is important for achieving high $\mathcal{Q}$ and ZT. However at the same time $\gamma_{ep} \gtrsim \gamma_e$ should preferably hold. If the NWs themselves do not ensure a large enough γ_{ep}, the use of a substrate providing phonons is to be envisaged. Yet, this will add a detrimental contribution K^{sub} to K^{ph}. In general the substrate cross-section (Σ^{sub}) will be substantially larger that the NWs one ($M\Sigma^{nw}$). Thus, even for a good thermal insulator such as SiO_2, with thermal conductivity $\kappa^{sub} \approx 0.7\,\mathrm{W/(K.m)}$ at $T \approx 100\,\mathrm{K}$ [29], $Z/Z_e = [1 + (\kappa^{sub}\Sigma^{sub} + M\kappa_0^{nw}\Sigma^{nw})/M\kappa_0^e\Sigma^{nw}]^{-1} \ll 1$. Better ratios Z/Z_e could be obtained for substrates with lower K^{sub} (Silica aerogels [30], porous silica [31], very thin substrate layer) but they will not necessary guarantee a good value of γ_{ep} (and hence of Z_e). Clearly, finding a balance between a large γ_{ep} and a low K^{ph} is a material engineering optimization problem. Though the presence of a substrate appears detrimental to the device efficiency, we shall now see how it could be used for a different purpose.

Hot spots cooling. Hereafter, we consider the deposited setup sketched in Fig. 1(b) and assume a constant temperature T everywhere. An intriguing feature of this setup is the possibility to generate/control hot and cold spots close to the substrate boundaries by applying a bias $\delta\mu/e$. This effect is a direct consequence of the heat exchange mechanism between electrons in the NWs and phonons in the substrate. Indeed, given a pair of localized states i and j inside a NW, with energies E_i and E_j respectively, the heat current absorbed from (or released to) the phonon bath by an electron in the transition $i \to j$ is $I_{ij}^Q = (E_j - E_i)\,I_{ij}^N$, I_{ij}^N being the hopping

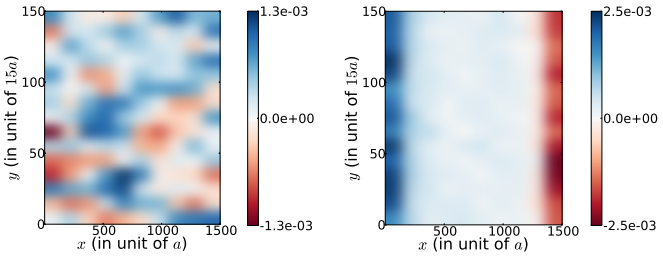

FIG. 3. (Color online) Map of the local heat exchanges $\mathcal{I}^Q_{x,y}$ between the NWs and the phonon bath (substrate), in unit of $t^2/\hbar$, at the band center ($V_g = 0$, left) and near the lower band edge ($V_g = 2.25t$, right). When phonons are absorbed by NWs charge carriers in the small area of size Λ^2_{ph} around (x, y), $\mathcal{I}^Q_{x,y} > 0$ and the substrate below is locally cooled down (blue). When phonons are released, $\mathcal{I}^Q_{x,y} < 0$ and the substrate is locally heated up (red). Data are for $M = 150$ NWs of length $L = 1500a$ with interspacing $15a$. Parameters: $k_BT = 0.25t$, $\Lambda_{ph} = 150a$, $W = t$, $\gamma_e = \gamma_{ep} = t/\hbar$ and $\delta\mu = 10^{-3}t$.

particle current between i and j [21]. The overall hopping heat current through each localized state i is then found by summing over all but the i-th states:

$$I^Q_i = \sum_j I^Q_{ij} = \sum_j (E_j - E_i)\, I^N_{ij} \qquad (2)$$

with the convention that I^Q_i is positive (negative) when it enters (leaves) the NWs at site i. Since the energy levels E_i are randomly distributed, the I^Q_i's (and in particular their sign) fluctuate from site to site (see Supplemental Material for an illustration). The physically relevant quantities are however not the I^Q_i's, rather their sum within an area $\Lambda_{ph} \times \Lambda_{ph}$, where Λ_{ph} is the phonons' thermalization length in the substrate (i.e. the length over which a *local* substrate temperature can be defined). Given a point (x, y) and a $\Lambda_{ph}\times\Lambda_{ph}$ area centered around it, such sum is denoted $\mathcal{I}^Q_{x,y}$. If $\mathcal{I}^Q_{x,y} > 0$ [< 0], a volume Λ^3_{ph} of the substrate beneath (x, y) is cooled [heated] [32]. Deeper than Λ_{ph} away from the surface, the equilibrium temperature T is reached.

Fig. 3 shows how $\mathcal{I}^Q_{x,y}$ depends on the coordinates x, y in the two-dimensional parallel NW array. Data are plotted having estimated $a \approx 3.2\,\text{nm}$, $t/k_B \approx 150\,\text{K}$, and $\lambda_{ph} \approx 480\,\text{nm} \approx 150a$ for SiO_2 substrate at the temperature considered, $T = 0.25t \approx 37.5\,\text{K}$. The estimates are discussed in the Supplemental Material. Two cases are compared in the figure: on the left, the situation in the absence of a gate voltage, when charge carriers tunnel into/out of NWs at the impurity band *center*; on the right, the opposite situation when a large gate voltage is applied in order to inject/extract carriers at the band *bottom*. All other parameters are fixed. In the first case, the heat map shows puddles of positive and negative $\mathcal{I}^Q_{x,y}$, corresponding respectively to cooled and heated regions in the substrate below. They are the signature of random absorption and emission of substrate phonons by the charge carriers, all along their propagation through the NWs around the band center. In the second case, the regions of positive and negative $\mathcal{I}^Q_{x,y}$ are respectively confined to the NWs entrance and exit. This is due to the fact that charge carriers entering the NWs at μ around the band bottom find available states to jump to (at a distance L_M in space and Δ in energy, $L_M \approx 10a$ and $\Delta \approx 1.1t$ here) only *above* μ. Therefore, they need to absorb phonons to reach higher energies states (blue region). After a few hops, having climbed at higher energies, they continue propagating with equal probabilities of having upward/downward energy hops (white region). On reaching the other end they progressively climb down, i.e. release heat to the substrate (red region), until they reach μ and tunnel out into the right reservoir. As a consequence, the substrate regions below the NWs extremities are cooled on the source side and heated on the drain side (see Fig. 1(b)).

We point out that the maximum values of $\mathcal{I}^Q_{x,y}$ are roughly of the same order of magnitude with or without the gate (see scale bars in Fig. 3). The advantage of using a gate is the ability to split the positive and negative $\mathcal{I}^Q_{x,y}$ regions into two well separated spots at the NWs extremities. One can then imagine to exploit the cold spot in the substrate to cool down a hot spot of an electronic circuit put in close proximity. Let us also stress that the assumption of elastic tunneling processes between the electrodes and the NWs is not necessary to observe the gate-induced hot/cold spots. The latter arise from the "climbing" up/down in energy that charge carriers, at μ far into the electrodes, must undergo in order to hop through the NWs (hopping transport being favored around the impurity band center in the NWs). Though in our model heat exchanges take place only inside the NWs, phonon emission/absorption will actually take place also at the electrodes' extremities, roughly within an inelastic relaxation length from the contacts. This has clearly no qualitative impact, as it only amounts to a slight shift/smearing of the hot/cold spots. We finish the discussion by giving an order of magnitude of the cooling power obtained in Fig. 3. Assuming again $t/k_B \approx 150\,\text{K}$, and $\Lambda_{ph} = 480\,\text{nm}$, we find that a value of $\mathcal{I}^Q_{x,y} = 10^{-3}(t^2/\hbar)$ in Fig. 3 corresponds to a cooling power density of the order of $2.10^{-10}\,\text{W}.\mu\text{m}^{-2}$. We underline that this order of magnitude is obtained for a given set of parameters (in particular for an infinitesimal bias $\delta\mu = 10^{-3}t$ that guarantees to remain in the linear response regime). It should not be taken in the strict sense but only as a benchmark value to fix ideas.

Conclusion. We studied arrays of doped semiconductor, parallel NWs in the FET configuration, focusing on the activated regime where charge transport between localized states is thermally assisted by phonons. By tuning the electrochemical potential μ near the band edges of the NW impurity band, we showed how to take advantage of electron-phonon coupling for energy harvesting

and hot spot cooling. A natural extension of this work would be to go beyond the linear response regime in order to reach larger output powers.

Acknowledgment. This work was supported by CEA within the DSM-Energy Program (project E112-7-Meso-Therm-DSM). We thank O. Bourgeois and Y. Imry for stimulating discussions.

[1] L. D. Hicks and M. S. Dresselhaus, Phys. Rev. B **47**, 16631 (1993)
[2] B. M. Curtin, E. W. Fang, and J. E. Bowers, J. Electron. Mat. **41**, 887 (2012)
[3] C. Blanc, A. Rajapbour, S. Volz, T. Fournier, and O. Bourgeois, Appl. Phys. Lett. **103**, 043109 (2013)
[4] Y. M. Brovman, J. P. Small, Y. Hu, Y. Fang, C. M. Lieber, and P. Kim, arXiv:1307.0249(2013)
[5] A. Stranz, A. Waag, and E. Peiner, J. Electron. Mat. **42**, 2233 (2013)
[6] S. Karg, P. Mensch, B. Gotsmann, H. Schmid, P. D. Kanungo, H. Ghoneim, V. Schmidt, M. T. Björk, V. Troncale, and H. Riel, J. Electron. Mat. **42**, 2409 (2013)
[7] S. Roddaro, D. Ercolani, M. A. Safeen, S. Suomalainen, F. Rossella, F. Giazotto, L. Sorba, and F. Beltram, Nano Lett. **13**, 3638 (2013)
[8] J. Moon, J.-H. Kim, Z. Chen, J. Xiang, and R. Chen, Nano Lett. **13**, 1196 (2013)
[9] Y. Tian, M. R. Sakr, J. M. Kinder, D. Liang, M. J. MacDonald, R. L. J. Qiu, H.-J. Gao, and X. P. A. Gao, Nano Lett. **12**, 6492 (2012)
[10] A. I. Hochbaum, R. Chen, R. D. Delgado, W. Liang, E. C. Garnett, M. Najarian, A. Majumdar, and P. Yang, Nature **451**, 163 (2008)
[11] M. Z. Atashbar, D. Banerji, S. Singamaneni, and V. Bliznyuk, Nanotechnology **15**, 374 (2004)
[12] R. Yerushalmi, Z. A. Jacobson, J. C. Ho, Z. Fan, and A. Javey, Appl. Phys. Lett. **91**, 203104 (2007)
[13] M. C. Wang and B. D. Gates, Materials Today **12**, 34 (2009)
[14] G. Zhang, K. Tateno, H. Gotoh, and H. Nakano, Nanotechnology **21**, 095607 (2010)
[15] D. Davila, A. Tarancon, M. Fernandez-Regulez, C. Calaza, M. Salleras, A. S. Paulo, and L. Fonseca, J. Micromech. Microeng. **21**, 104007 (2011)
[16] R. A. Farrell, N. T. Kinahan, S. Hansel, K. O. Stuen, N. Petkov, M. T. Shaw, L. E. West, V. Djara, R. J. Dunne, O. G. Varona, P. G. Gleeson, J. S.-J, H.-Y. Kim, M. M. Koleśnik, T. Lutz, C. P. Murray, J. D. Holmes, P. F. Nealey, G. S. Duesberg, V. Krstić, and M. A. Morris, Nanoscale **4**, 3228 (2012)
[17] S. Pregl, W. M. Weber, D. Nozaki, J. Kunstmann, L. Baraban, J. Opitz, T. Mikolajick, and G. Cuniberti, Nano Research **6**, 381 (2013)
[18] B. Shklovskii and A. Efros, *Electronic Properties of Doped Semiconductors* (Springer-Verlag, Berlin, 1984)
[19] J.-H. Jiang, O. Entin-Wohlman, and Y. Imry, Phys. Rev. B **85**, 075412 (2012)
[20] J.-H. Jiang, O. Entin-Wohlman, and Y. Imry, Phys. Rev. B **87**, 205420 (2013)
[21] R. Bosisio, C. Gorini, G. Fleury, and J.-L. Pichard, (accepeted for publication in New J. of Phys.) arXiv:1403.7475(2014)
[22] A. Miller and E. Abrahams, Phys. Rev. **120**, 745 (1960)
[23] A. Vassighi and M. Sachdev, *Thermal and Power Management of Integrated Circuits* (Springer, 2006)
[24] V. Ambegaokar, B. I. Halperin, and J. S. Langer, Phys. Rev. B **4**, 2612 (1971)
[25] H. Callen, *Thermodynamics and an Introduction to Thermostatics* (John Wiley and Sons, New York, 1985)
[26] We estimated t by comparing the band width $4t + W$ in our model to the typical width of the impurity band in highly doped Silicon NWs (see for instance Ref. [33]). Note that the NWs are then depleted by field effect.
[27] G. Benenti, G. Casati, T. Prosen, and K. Saito, arXiv:1311.4430(2013)
[28] D. Li, Y. Wu, P. Kim, L. Shi, P. Yang, and A. Majumdar, Appl. Phys. Lett. **83**, 2934 (2003)
[29] M.-T. Hung, C.-C. Wang, J.-C. Hsu, J.-Y. Chiou, S.-W. Lee, T. M. Hsu, and P.-W. Li, Appl. Phys. Lett. **101**, 251913 (2012)
[30] P. Hopkins, B. Kaehr, L. M. Phinney, T. P. Koehler, A. M. Grillet, D. Dunphy, F. Garcia, and C. J. Brinker, J. Heat Transfer **133**, 061601 (2011)
[31] P. Scheuerpflug, M. Hauck, and J. Fricke, J. Non-Cryst. Solids **145**, 196 (1992)
[32] Practically, we map the 2D parallel NW array onto a square grid, and for each square of size Λ_{ph}^2 we calculate the net heat current entering the NWs. For better visibility, data are then smoothed (with a standard gaussian interpolation) to produce the heat map shown in Fig. 3.
[33] F. Salleh and H. Ikeda, Advanced Materials Research **222**, 197 (2011)